

MODEL-BASED INVERSE HALFTONING WITH WAVELET-VAGUELETTE DECONVOLUTION

Ramesh Neelamani, Robert Nowak, and Richard Baraniuk

Rice University, Houston, TX 77005, USA

ABSTRACT

In this paper, we demonstrate based on the linear model of [1, 2] that inverse halftoning is equivalent to the well-studied problem of deconvolution in the presence of colored noise. We propose the use of the simple and elegant wavelet-vaguelette deconvolution (WVD) algorithm to perform the inverse halftoning. Unlike previous wavelet-based algorithms, our method is model-based; hence it is adapted to different error diffusion halftoning techniques. Our inverse halftoning algorithm consists of inverting the convolution operator followed by denoising in the wavelet domain. For signals in a Besov space, our algorithm possesses asymptotically (as the number of samples $\rightarrow \infty$) near-optimal rates of error decay. Hence for images in a Besov space, it is impossible to improve significantly on the inverse halftoning performance of the WVD algorithm at high resolutions. Using simulations, we verify that our algorithm outperforms or matches the performances of the best published inverse halftoning techniques in the mean square error (MSE) sense and also provides excellent visual performance.

1. INTRODUCTION

Halftoning is a common technique used by printers to render a continuous-tone gray-scale image using only black or white dots. Inverse halftoning is the process of retrieving the continuous-tone image from a given halftone. Applications of inverse halftoning include enhancement and compression of facsimile images [3]. In this paper, we focus on inverse halftoning images that are halftoned using the popular error diffusion techniques such as those of Floyd et al. [4], and Jarvis et al. [5] (hereby referred to as Floyd and Jarvis respectively).

Recently, Kite et al. proposed an accurate linear model for error diffusion halftoning [1, 2] (see Figure 1). Using this linear model, we can infer that inverse halftoning is equivalent to the well-studied problem of deconvolution.

Like conventional deconvolution algorithms, many conventional inverse halftoning algorithms operate in the Fourier domain.¹ For eg., Gaussian lowpass filtering [6] can be viewed as performing Fourier-domain deconvolution. However, Fourier-domain inverse halftoning techniques such as

Gaussian lowpass filtering provide unsatisfactory solutions because the Fourier-domain is not well-suited to represent signals such as images which contain spatially localized features such as edges.

In contrast to the Fourier transform, the wavelet transform is well-suited to represent spatially localized signals such as images. This property has been leveraged into powerful, spatially adaptive, signal estimation algorithms that are based on simply shrinking the wavelet coefficients of the noisy signal [7, 8].

These desirable properties of the wavelet transform were first exploited in inverse halftoning by J. Luo et al. [9] using edge-adapted noise attenuation in the wavelet subbands. Xiong et al. [10] extended this algorithm using non-orthogonal, redundant wavelets to obtain marginally better results for error diffused halftones. However, both these algorithms rely on adapting the parameters in the algorithm empirically.

In this paper, we exploit the equivalence between inverse halftoning and deconvolution to come up with an optimal wavelet-based inverse halftoning algorithm. We exploit Donoho's wavelet-vaguelette decomposition algorithm for deconvolution to inverse halftone error diffused images. The proposed algorithm consists of the following steps (see Figure 2):

1. Invert the convolution operator that is determined by the linear error diffusion model of [1, 2].
2. Use wavelet-domain thresholding to eliminate the residual blue noise.

For images in a Besov space, this simple technique attains near-optimal rates of error decay as the resolution increases (i.e., as the number of samples $\rightarrow \infty$).

Section 2 describes the linear model for error diffused halftoning. Section 3 clarifies the equivalence between inverse halftoning and deconvolution, and analyzes Fourier-domain inverse halftoning techniques. Sections 4 and 5 discuss the proposed inverse halftoning algorithm and its optimality properties respectively. Section 6 illustrates the performance of the proposed algorithm. Section 7 provides the conclusions of our research.

2. LINEAR MODEL FOR ERROR DIFFUSION

Figure 1 (a) illustrates the block diagram for error diffused halftoning process. Here $x(n)$ and $y(n)$ denote the pixels of the continuous-tone gray scale image and the halftoned image, respectively. The image $x'(n)$ is obtained after the error $e(n)$

This work was supported by the NSF grants CCR-9973188 and MIP-9701692, DARPA/AFOSR grant F49620-97-1-0513, ONR grant N00014-99-1-0219, ARO grant DAAD19-99-1-0349, and Texas Instruments.

Email: neelsh@rice.edu, nowak@rice.edu, richb@rice.edu

Web: www.dsp.rice.edu

¹Note that the Fourier transform diagonalizes convolution operators

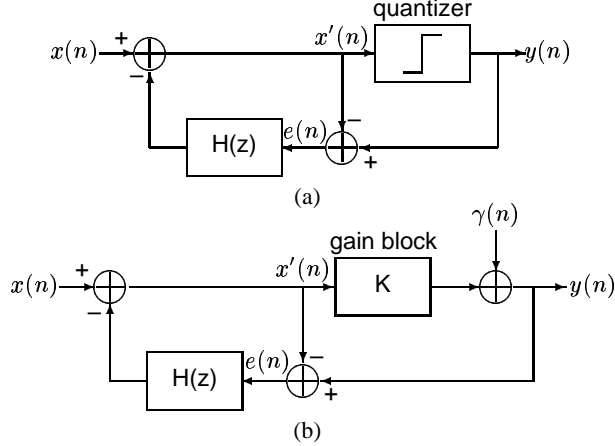


Fig. 1. (a) Error diffused halftoning is a nonlinear process due to the presence of the quantizer. Symbols $x(n)$ and $y(n)$ denote the pixels of the continuous-tone gray scale image and the halftoned image, respectively. The error filter $H(z)$ characterizes the type of error diffusion. (b) Linearized model [1, 2] approximates the quantizer with a cascade of a gain block K and additive white noise samples $\gamma(n)$. For any given error diffusion technique, the gain K is almost constant for all images. However, K changes to adapt the model to the different error diffusion techniques. For example, $K \approx 2$ for Floyd et al. [4] and $K \approx 4.5$ for Jarvis et al. [5].

is diffused over a causal neighborhood of $x(n)$ by the error filter $H(z)$. Different error diffusion techniques such as Floyd and Jarvis are obtained using appropriate error filters. Due to the presence of the quantizer, error diffusion is a nonlinear technique.

Recently, Kite et al. proposed an accurate linear model for halftoning using error diffusion [1, 2]. As shown in Figure 1(b), this model approximates the effects of quantization using a gain block K followed by the addition of white noise $\gamma(n)$. The halftoned image $y(n)$ can then be written in terms of the continuous-tone input $x(n)$ and the additive white noise $\gamma(n)$ as

$$Y(z) = P(z)X(z) + Q(z)\Gamma(z), \quad (1)$$

where $Y(z)$, $X(z)$, and $\Gamma(z)$ are the z -transforms of $y(n)$, $x(n)$, and $\gamma(n)$ respectively; and $P(z) := \frac{K}{1+(K-1)H(z)}$ and $Q := \frac{1-H(z)}{1+(K-1)H(z)}$ are linear time-invariant (LTI) filters determined by the error diffusion technique. Kite et al. found that the gain K is almost constant for different images, but varied with the error diffusion technique [1, 2]. For example, $K \approx 2$ for Floyd, while $K \approx 4.5$ for Jarvis. This linear model accurately predicts the noise behavior and explains the edge sharpening effects seen in the various error diffusion techniques.

3. CONVENTIONAL INVERSE HALFTONING

According to the model of [1, 2], the halftone Y consists of X convolved with P and corrupted by colored noise $Q\Gamma$ (see (1)). Since P and Q are LTI filters, estimating X from Y using inverse halftoning is equivalent to deconvolution in the presence of colored noise, a well-studied problem.

Deconvolution techniques formally consist of the following steps:

1. Invert the convolution operator P to obtain a noisy estimate of the input signal.

$$\tilde{X}(z) := P^{-1}(z)Y(z) = X(z) + P^{-1}(z)Q(z)\Gamma(z). \quad (2)$$

2. Attenuate the noise $P^{-1}(z)Q(z)\Gamma(z)$ in $\tilde{X}(z)$ to obtain an estimate of the input signal. Since (1) and (2) are interchangeable, deconvolution is also equivalent to denoising (i.e., attenuating) colored noise.

Conventional techniques perform Step 2 in the Fourier-domain because the noise Fourier components are uncorrelated, since the Fourier transform diagonalizes convolution operators.

However, since the Fourier basis elements have support over the entire spatial domain, the Fourier-domain is unsuited to represent images with edges and ridges. Consequently, distortion of localized features such as edges is a commonly observed drawback of Fourier-domain deconvolution techniques. Inverse halftoning using Gaussian low-pass filtering [6] can be interpreted as one form of Fourier-domain deconvolution; hence it inevitably over-smoothes edges.

4. INVERSE HALFTONING WITH WAVELET-VAGUELETTE DECONVOLUTION (WVD)

In contrast to the Fourier transform, the wavelet transform is well-suited to deal with signals and images containing spatially localized features such as edges. Wavelets provide economical representations for such signals which belong to a Besov space [11, 12], i.e., the wavelet expansion captures most of the signal energy using a few large wavelet coefficients.

Motivated by the economy of wavelet representations, Donoho proposed the wavelet-vaguelette decomposition algorithm to solve a special class of linear inverse problems [12]. With a slight abuse of notation, we will refer to the wavelet-vaguelette decomposition as applied to deconvolution as wavelet-vaguelette deconvolution (WVD). For estimating signals in Besov spaces, such an algorithm exhibits asymptotically (as the number of samples of the image increases) near-optimal rates of error decay for dilation-homogeneous operators [12, 13].²

In this paper, we propose the use of WVD as a near-optimal technique to perform inverse halftoning. Our WVD inverse halftoning algorithm can formally be described as follows (see Figure 2):

1. As in (2), obtain a unbiased but noisy estimate \tilde{x} of the input signal.
2. In contrast to Fourier-domain deconvolution, employ wavelet-domain denoising (eg. thresholding [12]) to obtain the inverse halftoned estimate \hat{x} .

In contrast to the wavelet-based inverse halftoning method of [10], our inverse halftoning algorithm is model-based. Hence, by simply using the appropriate filters P and Q , our technique can be adapted to the different error diffusion techniques such as Floyd and Jarvis.

²An operator h is dilation-homogeneous if $h(t) \otimes y(at) = a^{-\nu} |a| h(at) \otimes y(at)$, where \otimes denotes convolution.

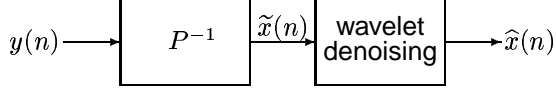


Fig. 2. Inversion half-toning with WVD: The algorithm inverts the convolution operator $P = \frac{\kappa}{1+(\kappa-1)H}$ to obtain a noisy estimate $\tilde{x}(n)$ of the input signal. Wavelet-domain denoising subsequently attenuates the noise in $\tilde{x}(n)$ and obtains the inverse half-toned estimate $\hat{x}(n)$.

5. ASYMPTOTIC OPTIMALITY OF INVERSE HALFTONING WITH WVD

To prove the optimality of the WVD inverse half-toning algorithm, we assume that the noise $\gamma(n)$ is Gaussian. At all scales except the finest scale, the noise histograms appeared Gaussian. Since the variance of noise in the finest scale is so high compared to the average energy of a typical desired signal, even ideal estimation adapted to the actual distribution of the noise will almost completely obliterate the signal in the finest scale. Hence assuming Gaussian noise in the finest scale will not significantly alter the performance of any algorithm.

In practice, the original image being half-toned is typically corrupted with some noise (eg., scanner noise). We assume that this noise $\delta(n)$ is white Gaussian with variance $c^2\sigma^2$, where c is a positive constant and σ^2 is the variance of $\gamma(n)$. The signal model in (1) is now modified to

$$Y(z) = P(z)(X(z) + \Delta(z)) + Q(z)\Gamma(z), \quad (3)$$

where $\Delta(z)$ is the z -transform of $\delta(n)$. The noisy signal after step 1 in the WVD inverse half-toning algorithm outlined in Section 4 is given by

$$\tilde{X}(z) = X(z) + \Delta(z) + P^{-1}(z)Q(z)\Gamma(z). \quad (4)$$

The power spectrum of the coloring noise in (4) is given by $\sigma^2(c^2 + |P^{-1}Q|^2)$. It is easily verified that

$$C_1 < \sigma^2(c^2 + |P^{-1}Q|^2) < C_2, \quad (5)$$

where C_1 and C_2 are strictly positive constants since $|P^{-1}Q|^2$ is bounded.

We can now invoke the optimality of signal estimation in the presence of white Gaussian noise using wavelet-domain thresholding from [7] to infer the optimality of WVD inverse half-toning algorithm. Consider two cases where the signal X corrupted by white Gaussian noise Λ_i with variance C_i is observed as Y_i , i.e., $Y_i = X + \Lambda_i$ for $i = 1, 2$. Let $R_i(N)$ be the rate of asymptotic error decay attained by using wavelet-domain thresholding to estimate the signal X from Y_i , where N is the number of samples. Let $R_{\text{IHT}}(N)$ be the rate of asymptotic error decay attained by the WVD inverse half-toning algorithm. From (5), since the variance of the effective colored noise encountered in inverse half-toning at any frequency is bounded by C_1 and C_2 , we can bound $R_{\text{IHT}}(N)$ as $R_1 \geq R_{\text{IHT}} \geq R_2$. When the signal X belongs to a Besov space, from [7], R_1 and R_2 are within a $\log(N)$ factor of the best error decay rate achievable by any estimation algorithm. Further, since $R_1 = R_2$, we can infer that the WVD inverse

Table 1. PSNR of different inverse half-toning algorithms.

Inverse half-toning algorithm	PSNR (dB)	
	<i>lena</i>	<i>peppers</i>
Gaussian [6]	28.6	27.6
Kernel [15]	32.0	30.2
Gradient [16]	31.3	31.4
Wavelet denoising [10]	31.7	30.7
WVD	31.9	31.0

half-toning algorithm possesses near-optimal asymptotic rates of error decay. Hence for images in a Besov space, it is impossible to significantly improve upon performance of the WVD inverse half-toning algorithm as the resolution N increases.

6. RESULTS

We illustrate the performance of our WVD inverse half-toning algorithm using 512×512 *lena* and *peppers* images half-toned using the Floyd algorithm [4]. To perform wavelet-domain denoising (Step 2) in the WVD algorithm, we use a redundant, shift-invariant wavelet basis; this yields significantly improved estimate by averaging over all possible shifts of the observation [14]. We quantify the performance of our algorithm by measuring the peak signal-to-noise ratio $PSNR := 20 \log_{10} \frac{512 \times 255}{\|\hat{x} - x\|_2}$ for an 512×512 image with \hat{x} the estimate.

Table 1 summarizes the performance of the WVD algorithm compared to Gaussian filtering [6], kernel estimation [15], gradient estimation [16], and wavelet denoising with edge-detection [10] inverse half-toning techniques. We can see that the WVD inverse half-toning algorithm outperforms or equals the best published results. Figure 3 demonstrates that the WVD algorithm has excellent visual performance as well.

7. CONCLUSIONS

Using the linear error diffusion model of [1, 2], we demonstrate that inverse half-toning is equivalent to deconvolution in the presence of colored noise. Exploiting this equivalence, we propose a new inverse half-toning algorithm based on the simple and elegant wavelet-vaguelette deconvolution (WVD) algorithm. Since our algorithm is model-based, it is tunable to the different error diffusion half-toning techniques. The algorithm yields state-of-the-art performance in the mean square error sense and visually.

Significantly, for signals in a Besov space, our algorithm enjoys asymptotically (as the number of samples $\rightarrow \infty$) near-optimal rates of error decay. Consequently, for images in a Besov space, it is impossible to significantly improve on the performance of our algorithm at high resolutions.

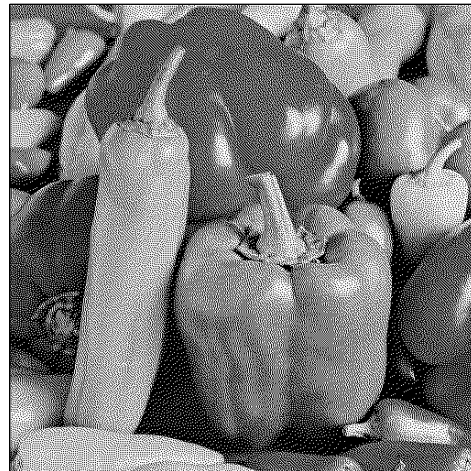
8. REFERENCES

- [1] T. D. Kite, B. L. Evans, A. C. Bovik, and T. L. Sculley, "Digital half-toning as 2-D delta-sigma modulation," *Proc. IEEE Int. Conf. Image Processing — ICIP '97*, vol. 1, pp. 799–802, Oct. 26–29 1997.
- [2] T. D. Kite, B. L. Evans, A. C. Bovik, and T. L. Sculley, "Modeling and quality assessment of half-toning by

- error diffusion," *IEEE Trans. Image Processing*, vol. 9, pp. 909–922, May 2000.
- [3] M. Y. Ting and E. A. Riskin, "Error-diffused image compression using a binary-to-gray scale decoder and predictive pruned tree-structured vector quantization," *IEEE Trans. Image Processing*, vol. 3, pp. 854–857, Nov. 1994.
- [4] R. W. Floyd and L. Stienberg, "An adaptive algorithm for spatial grayscale," *Proc. SID*, vol. 17, no. 2, pp. 75–77, 1976.
- [5] J. Jarvis, C. Judice, and W. Ninke, "A survey of techniques for the display of continuous tone pictures on bilevel displays," *Comp. Graph and Image Proc.*, vol. 5, pp. 13–40, 1976.
- [6] S. Hein and A. Zakhor, "Halftone to continuous-tone conversion of error-diffusion coded images," *IEEE Trans. Image Processing*, vol. 4, pp. 208–216, Feb. 1995.
- [7] D. L. Donoho and I. M. Johnstone, "Ideal spatial adaptation via wavelet shrinkage," *Biometrika*, vol. 81, pp. 425–455, 1994.
- [8] D. L. Donoho, "Nonlinear wavelet methods for recovery of signals, densities, and spectra from indirect and noisy data," in *Different Perspectives on Wavelets*, vol. 47 of *Proc. Symp. Appl. Math.*, pp. 173–205, American Mathematical Society, 1993.
- [9] J. Luo, R. DeQueiroz, and Z. Fan, "A robust technique for image descreening based on the wavelet transform," *IEEE Trans. Signal Processing*, vol. 46, pp. 1179–1184, April 1998.
- [10] Z. Xiong, M. T. Orchard, and K. Ramchandran, "Inverse halftoning using wavelets," *IEEE Trans. Signal Processing*, vol. 8, pp. 1479–1482, Oct. 1999.
- [11] R. A. DeVore, B. Jawerth, and B. J. Lucier, "Image compression through wavelet transform coding," *IEEE Trans. Inform. Theory*, vol. 38, pp. 719–746, Mar. 1992.
- [12] D. L. Donoho, "Nonlinear solution of linear inverse problems by Wavelet-Vaguelette Decomposition," *App. Comp. Harmonic Anal.*, vol. 2, pp. 101–126, 1995.
- [13] I. M. Johnstone and B. W. Silverman, "Wavelet threshold estimators for data with correlated noise," *J. Royal Stat. Soc. B*, no. 59, pp. 319–351, 1997.
- [14] R. Coifman and D. Donoho, "Translation invariant denoising," in *Wavelets and Statistics* (A. Antoniadis, ed.), Springer, 1995.
- [15] P. Wong, "Inverse halftoning and kernel estimation for error diffusion," *IEEE Trans. Image Processing*, vol. 6, pp. 486–498, Apr. 1995.
- [16] T. D. Kite, N. Damera-Venkata, B. L. Evans, and A. C. Bovik, "A high quality, fast inverse halftoning algorithm for error diffused halftones," *Proc. IEEE Int. Conf. Image Processing — ICIP '98*, vol. 2, pp. 59–63, Oct. 4–7 1998.



(a)



(b)



(c)

Fig. 3. (a) Original peppers image. (b) Floyd halftone. (c) The WVD algorithm not only provides excellent PSNR performance, but also excellent visual performance.